Journal of
Micro/Nanolithography, MEMS, and MOEMS

SPIEDigitalLibrary.org/jm3

Reaction-diffusion power spectral density

Chris A. Mack

SPIE

Reaction-diffusion power spectral density

Chris A. Mack
Lithoguru.com
1605 Watchhill Road
Austin, Texas 78703
E-mail: chris@Lithoguru.com

Abstract. Characterization of a stochastic process in lithography, giving rise to photoresist line-edge roughness (LER), requires elucidation of the power spectral density (PSD) for that process. Thus, any analytical model for LER requires an analytical model for the PSD. Using a previously derived formulation for the reaction-diffusion autocorrelation function, the PSD can be derived from its Fourier transform. The resulting analytical expression for the reaction-diffusion PSD provides an interesting and useful form that will aid modeling work in LER prediction. Numerically calculating the PSD for the stochastic development rate shows that this same analytical expression approximately matches the simulation but with a correlation length that decreases as the amount of development noise increases. © *2012 Society of Photo-Optical Instrumentation Engineers (SPIE).* [DOI: 10.1117/1.JMM.11.4.043007]

Subject terms: stochastic resist; correlation length; power spectral density; reaction-diffusion; lithography simulation; line-edge roughness; linewidth roughness.

Paper 12070 received Jun. 26, 2012; revised manuscript received Aug. 22, 2012; accepted for publication Sep. 25, 2012; published online Oct. 20, 2012.

1 Introduction

Stochastic variations in photoresist exposure, reaction-diffusion, and development ultimately lead to sidewall surface roughness of the final photoresist features, described as line-edge roughness (LER) or linewidth roughness (LWR). Full characterization of the LER requires its description over the spectrum of roughness frequency components, most commonly using the power spectral density (PSD). While a comprehensive model for LER formation in lithography does not yet exist, several pieces of the puzzle have been explored. For example, models for the prediction of the uncertainty in acid concentration after exposure of a chemically amplified resist have been developed for 193-nm[1] and extreme ultraviolet (EUV) resists.[2]

Reaction-diffusion results in a distribution of protected and deprotected polymer groups at the end of the post-exposure bake (PEB). This spatial distribution of the protecting group (the latent image after PEB) then leads to a development rate distribution that ultimately determines the final resist profile shape. Understanding the PSD of the latent image and the development rate distribution are important steps in a full understanding of the PSD behavior of LER. In Sec. 2, an analytical expression for the PSD of the effective acid concentration during PEB will be derived. That same expression will be shown to be applicable to the PSD of the protecting group concentration after PEB, under certain circumstances, in Sec. 3. Finally, in Sec. 4 the PSD of the development rate will be numerically evaluated.

The PSD of the stochastic distribution of development rates, while the final result of this paper, is only an intermediate result of the full development process. The surface-limited etching mechanism of resist dissolution will transform the stochastic development rates of the resist into a final rough surface on the sidewalls of the resist feature. The results presented in this paper thus can serve as an input to a dissolution/etching algorithm that in turn will predict the final surface roughness (the subject of future work).

2 Reaction-Diffusion PSD—the Effective Acid Concentration

The random distribution of acid after exposure of a chemically amplified resist is essentially uncorrelated (and thus its PSD will be flat—white noise) when ignoring such a correlating mechanism as speckle during 193-nm exposure,[3,4] or secondary electron generation for 13.5-nm exposure. Reaction-diffusion, where the acid diffuses and acts as a catalyst for a polymer deprotection reaction, adds correlation to the resulting uncertainty. One acid can deprotect multiple polymer sites; as a result, those deprotection reactions are not independent. In a previous study,[5,6] the autocorrelation function of the effective acid concentration during PEB for a chemically amplified resist ($\tilde{R}_{H_{\text{eff}}}$) was derived.

$$\tilde{R}_{H_{\text{eff}}}(\tau) = \frac{\int_{-\infty}^{\infty} R_{\text{PSF}}(s) R_{\text{PSF}}(s+\tau)\mathrm{d}s}{\int_{-\infty}^{\infty} [R_{\text{PSF}}(s)]^2 \mathrm{d}s}, \tag{1}$$

where τ is the radial distance from the origin, and the reaction-diffusion point spread function (R_{PSF}) has analytical forms in one, two, and three dimensions.

$$\begin{aligned}
1\text{-}D &: R_{\text{PSF}}(x) = 2\frac{\exp(-x^2/2\sigma_D^2)}{\sqrt{2\pi}\sigma_D} - \frac{|x|}{\sigma_D^2}\operatorname{erfc}\left(\frac{|x|}{\sqrt{2}\sigma_D}\right), \\
2\text{-}D &: R_{\text{PSF}}(r) = -\frac{1}{2\pi\sigma_D^2}\operatorname{Ei}\left(-\frac{r^2}{2\sigma_D^2}\right),\ r = \sqrt{x^2+y^2}, \\
3\text{-}D &: R_{\text{PSF}}(r) = \frac{1}{2\pi\sigma_D^3}\left[\frac{\sigma_D}{|r|}\operatorname{erfc}\left(\frac{|r|}{\sqrt{2}\sigma_D}\right)\right], r = \sqrt{x^2+y^2+z^2}
\end{aligned} \tag{2}$$

The effective acid concentration (H_{eff}) is the time average of the acid concentration during the bake and is the convolution of the initial acid concentration after exposure with the

reaction-diffusion point spread function.[7] Note that the PSD is simply the Fourier transform of the autocorrelation function, and in general, the resulting PSD will have different forms in different dimensions.[8]

While the integrals in Eq. (1) cannot be carried out analytically in any dimension, the Fourier transform of Eq. (1) can, yielding the PSD.

$$\mathrm{PSD}(f) = \mathrm{PSD}(0)\left(\frac{1 - e^{-(\pi\xi f)^2}}{(\pi\xi f)^2}\right)^2, \tag{3}$$

where the correlation length-like parameter ξ is related to the acid diffusion length σ_D by $\xi = \sqrt{2}\sigma_D$. The zero frequency PSD is calculated from Parseval's theorem.

$$\begin{aligned}
1-D\text{: } \mathrm{PSD}(0) &= \frac{3\sqrt{\pi}\xi\sigma_{H_{\mathrm{eff}}}^2}{8\left(\sqrt{2}-1\right)} \approx 1.60466\xi\sigma_{H_{\mathrm{eff}}}^2,\\
2-D\text{: } \mathrm{PSD}(0) &= \frac{\pi\xi^2\sigma_{H_{\mathrm{eff}}}^2}{2\ln 2} \approx 2.26618\xi^2\sigma_{H_{\mathrm{eff}}}^2,\\
3-D\text{: } \mathrm{PSD}(0) &= \frac{\pi^{3/2}\xi^3\sigma_{H_{\mathrm{eff}}}^2}{4(2-\sqrt{2})} \approx 2.37643\xi^3\sigma_{H_{\mathrm{eff}}}^2.
\end{aligned} \tag{4}$$

In the high frequency limit, where $\pi\xi f \gg 1$, we see that $\mathrm{PSD} \sim 1/f^4$, corresponding to a Hurst exponent of $\alpha = 0.5$ for the 3-D case.

Interestingly, the reaction-diffusion PSD is the same, to within a scale factor, for one, two, and three dimensions. This is not generally assumed to be the case. For example, it has been common to assume that a stretched exponential autocorrelation function can apply.[9,10]

$$\tilde{R}(s) = \sigma^2 e^{-(s/\xi_x)^{2\alpha}}. \tag{5}$$

For $\alpha = 0.5$, the resulting PSD can be analytically derived.[8] Letting d be the dimensionality of the problem,

$$\mathrm{PSD}_x(f) = \frac{a_d\sigma^2\xi_x^d}{\left[1 + (2\pi f\xi_x)^2\right]^{\frac{d+1}{2}}}, \tag{6}$$

where $a_1 = 2$, $a_2 = 2\pi$, and $a_3 = 8\pi$. For the 3-D case, this expression produces the high frequency $1/f^4$ behavior found for the reaction-diffusion PSD. For 1-D and 2-D problems, however, Eq. (6) predicts $1/f^2$ and $1/f^3$ behavior, respectively, while the reaction-diffusion PSD of Eq. (3) predicts a high frequency $1/f^4$ behavior for all dimensions.

Comparing the reaction-diffusion PSD of Eq. (3) to the 3-D version of Eq. (6), the frequency behavior can be made to match in the low-frequency regime, or in the high-frequency regime, but not both. Matching at low frequencies gives

$$\begin{aligned}
\mathrm{PSD}_x(0) = 8\pi\sigma^2\xi_x^3 &= \mathrm{PSD}_{\mathrm{RD}}(0) = \frac{\pi^{3/2}\xi^3\sigma^2}{4(2-\sqrt{2})},\\
\xi_x &= \xi\left[\frac{\sqrt{\pi}}{32\left(2-\sqrt{2}\right)}\right] \approx 0.4556\xi.
\end{aligned} \tag{7}$$

Matching at high frequencies gives

$$\xi_x = \xi\left[\frac{2(2-\sqrt{2})}{\sqrt{\pi}}\right] \approx 0.6610\xi. \tag{8}$$

In either case, the mid-frequency regime will not match, as seen in Fig. 1. The differences, while not dramatic, are noticeable.

3 Correlation Length

There is no universally accepted definition of correlation length (L_{corr}) that can pin down its value except to within a multiplicative factor. One definition, for example, is based on the frequency that reduces the PSD by a factor of 2

$$\mathrm{PSD}\left(f = \frac{1}{2\pi L_{\mathrm{corr}}}\right) = \frac{\mathrm{PSD}(0)}{2}. \tag{9}$$

By this definition, the correlation length of the reaction-diffusion system is related to ξ by $L_{\mathrm{corr}} = 0.5819\xi = 0.8229\sigma_D$ (for 1-D, 2-D, and 3-D). Another common definition, proposed by Stratonovich,[11] is the area under the autocorrelation function curve:

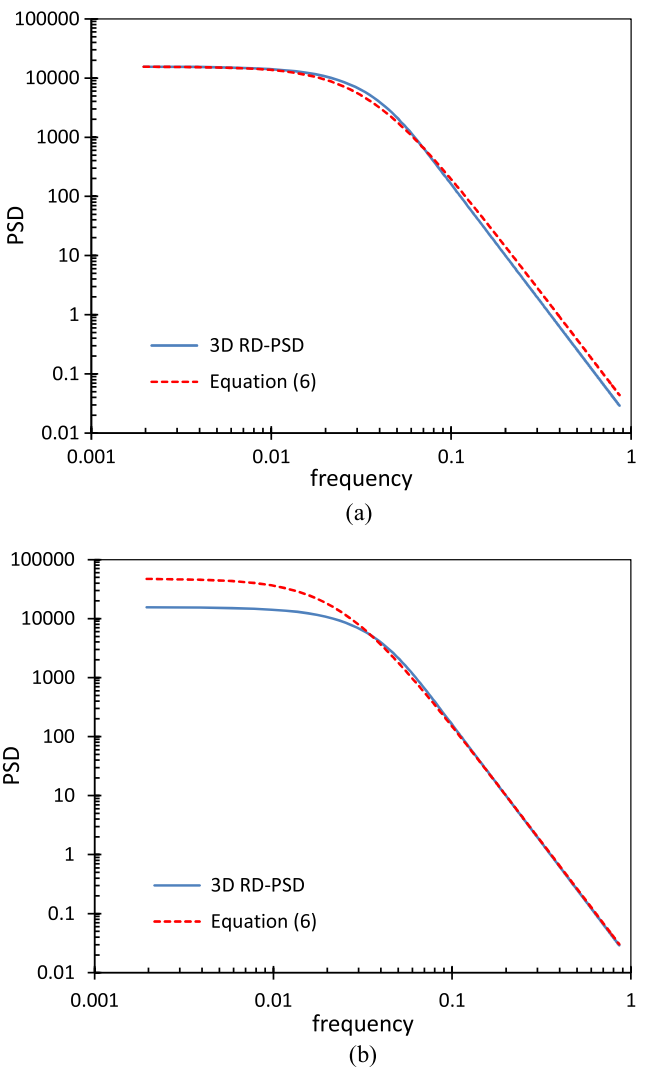

Fig. 1 Comparing the reaction-diffusion PSD and Eq. (6) in three dimensions for (a) matching low frequencies and (b) matching high frequencies.

$$L_{\text{corr}} = \int_0^\infty \tilde{R}\mathrm{d}s = \frac{1}{\sigma^2}\int_0^\infty F^{-1}\{\text{PSD}\}\mathrm{d}s, \tag{10}$$

where the autocorrelation function is assumed to be an even function of the distance s. The second integral can be simplified by changing the order of integration, giving a result that depends on the dimensionality of the problem

$$\begin{aligned}
1-D\text{: } L_{\text{corr}} &= \frac{\text{PSD}(0)}{2\sigma^2},\\
2-D\text{: } L_{\text{corr}} &= \frac{1}{\sigma^2}\int_{-\infty}^{\infty}\text{PSD}\mathrm{d}f,\\
3-D\text{: } L_{\text{corr}} &= \frac{1}{\sigma^2}\int_{-\infty}^{\infty} f\text{PSD}\mathrm{d}f.
\end{aligned} \tag{11}$$

Carrying out these calculations for the reaction-diffusion PSD,

$$\begin{aligned}
1-D\text{: } L_{\text{corr}} &= \frac{3\sqrt{\pi}}{16(\sqrt{2}-1)}\xi \approx 0.80233\xi,\\
2-D\text{: } L_{\text{corr}} &= \frac{\text{PSD}_{2D}(0)}{\text{PSD}_{1D}(0)} = \frac{4\sqrt{\pi}(\sqrt{2}-1)}{3\ \ln 2}\xi \approx 1.41225\xi,\\
3-D\text{: } L_{\text{corr}} &= \frac{\text{PSD}_{3D}(0)}{\text{PSD}_{2D}(0)} = \frac{\sqrt{\pi}\ \ln 2}{2(2-\sqrt{2})}\xi \approx 1.04865\xi.
\end{aligned} \tag{12}$$

Thus, depending on the definition used and the dimensionality of the problem, the correlation length is between 0.58ξ and 1.41ξ. It seems reasonable, therefore, to define the correlation length for the reaction-diffusion system as being synonymous with the parameter ξ.

4 Reaction-diffusion PSD—the Protecting Group Concentration

The relationship between the effective acid concentration and the relative concentration of protecting groups in the chemically amplified resist (m) is exponential, making calculation of the PSD for m difficult.

$$m = e^{-\alpha_f h_{\text{eff}}}, \tag{13}$$

where α_f is the amplification factor (with typical values between 1 and 2), equal to the amplification rate constant times the PEB time, and h_{eff} is the effective acid concentration relative to the initial photoacid generator concentration.[7] When the effective relative acid concentration near the resist line-edge is sufficiently small that a linear approximation to this exponential relationship is reasonable, the relative protecting group concentration will have a PSD of the same form as Eqs. (3) and (4), where the variance of the effective acid concentration is replaced by the variance of the relative protecting group concentration, σ_m^2.

For the more general case, numerical simulations can be used to explore the shape of the PSD of the relative protecting group concentration. Given a normally distributed random variable $h_{\text{eff}} \sim N(\mu_h, \sigma_h)$ and a desired PSD, how does one generate a random volume of $h_{\text{eff}}(x, y, z)$ on a regular grid? While there are several methods available, I prefer the approach proposed by Thorsos.[12] The goal is to create a grid of random numbers with a Gaussian distribution and with spatial correlations that would produce, on average, a given PSD. Thorsos described the algorithm in one dimension, which will be reproduced briefly here. Given N_x grid points with spacing Δx covering a distance $L_x = N_x\Delta x$, the relative effective acid concentration at the point $x_n = n\Delta x$ is given by

$$h_{\text{eff}}(x_n) = \mu_h + \frac{1}{L_x}\sum_{j=-N_x/2}^{N_x/2-1} F(f_j)e^{i2\pi f_j x_n}, \tag{14}$$

where this calculation is performed as the Fast Fourier Transform (FFT) of F on a grid of frequencies $f_j = j/L_x$. The function F, in turn, is calculated from the amplitude of the PSD (for $j \geq 0$):

$$F(f_j) = \sqrt{L_x\text{PSD}(f_j)}\begin{cases}(\eta_1 + i\eta_2)/\sqrt{2}, & j \neq 0, N_x/2\\ \eta_1, & j = 0, N_x/2\end{cases}, \tag{15}$$

where η_1 and η_2 are two independent $N(0,1)$ random numbers. Since $h_{\text{eff}}(x_n)$ must be real, the negative frequencies of F are obtained from a symmetry relationship: $F(f_{-j}) = F*(f_j)$.

The Thorsos algorithm can easily be extended to two and three dimensions, so long as care is taken to properly produce the boundary conditions (a purely real random number is used at the origin and at the outer edges of the volume) and the symmetry to result in a purely real h_{eff}. In two dimensions, this requires

$$\begin{aligned}
\text{Re}\{F(f_x, f_y)\} &= \text{Re}\{F(-f_x, -f_y)\},\\
\text{Re}\{F(-f_x, f_y)\} &= \text{Re}\{F(f_x, -f_y)\},\\
\text{Im}\{F(f_x, f_y)\} &= -\text{Im}\{F(-f_x, -f_y)\},\\
\text{Im}\{F(-f_x, f_y)\} &= -\text{Im}\{F(f_x, -f_y)\}.
\end{aligned} \tag{16}$$

In three dimensions,

$$\begin{aligned}
\text{Re}\{F(f_x, f_y, f_z)\} &= \text{Re}\{F(-f_x, -f_y, -f_z)\},\\
\text{Re}\{F(-f_x, f_y, f_z)\} &= \text{Re}\{F(f_x, -f_y, -f_z)\},\\
\text{Re}\{F(f_x, -f_y, f_z)\} &= \text{Re}\{F(-f_x, f_y, -f_z)\},\\
\text{Re}\{F(f_x, f_y, -f_z)\} &= \text{Re}\{F(-f_x, -f_y, f_z)\},\\
\text{Im}\{F(f_x, f_y, f_z)\} &= -\text{Im}\{F(-f_x, -f_y, -f_z)\},\\
\text{Im}\{F(-f_x, f_y, f_z)\} &= -\text{Im}\{F(f_x, -f_y, -f_z)\},\\
\text{Im}\{F(f_x, -f_y, f_z)\} &= -\text{Im}\{F(-f_x, f_y, -f_z)\},\\
\text{Im}\{F(f_x, f_y, -f_z)\} &= -\text{Im}\{F(-f_x, -f_y, f_z)\}.
\end{aligned} \tag{17}$$

The random m is produced by putting the random value of h_{eff} for each grid point into Eq. (13). Then, the resulting volume of random m was analyzed by extracting its PSD. Since the result is inherently spherically symmetric [dictated by the symmetry of Eq. (3)], the PSD as a function of the three spatial frequency dimensions was interpolated onto one radial-direction grid. This provides an added benefit of significant averaging for high spatial frequencies (though none for the lowest frequency). Further averaging is obtained

by repeating the numerical simulation numerous times and averaging the resulting PSDs.

For a Gaussian distribution of h_{eff}, the distribution of m will be log-normal, with mean and standard deviation given by

$$\langle m\rangle = e^{-\alpha_f \mu_h} e^{\alpha_f^2 \sigma_h^2/2}, \quad \sigma_m^2 = \langle m\rangle^2 (e^{\alpha_f^2 \sigma_h^2} - 1). \tag{18}$$

The shape of the PSD of m was explored in the 2-D case for $\sigma_m = 0.05$ and varying $\langle m\rangle$, using $\alpha_f = 1.5$. The resulting numerical PSDs (the average of 2000 trials for each set of parameters) matched Eqs. (3) and (4) extremely well so long as μ_h was not too close to 0 or 1. In particular, a good match to the PSD expression occurred when

$$\mu_h - 3\sigma_h > 0 \quad \text{and} \quad \mu_h + 4\sigma_h < 1. \tag{19}$$

Note that these are also the approximate constraints on describing the distribution of h_{eff} as Gaussian. Also note that under these conditions and for $\sigma_m = 0.05$ or less, the log-Normal distribution for m is approximately Normal in shape.

5 Development Rate PSD

Dissolution rate uncertainty will inevitably result from uncertainty in the underlying inhibitor concentration. Consider a simple development rate function[13]

$$r = r_{\max} \frac{(a+1)(1-m)^n}{a + (1-m)^n} + r_{\min},$$
$$a = \frac{(n+1)}{(n-1)}(1 - m_{\text{th}})^n, \tag{20}$$

where r is the development rate, and $r_{\max}$, $r_{\min}$, n, and m_{th} are model parameters. Here, we will neglect $r_{\min}$ as small compared to the development rate in the region of interest. The edge of a photoresist feature will necessarily have a protection level that is near the knee of the development rate curve, so that $m > m_{\text{th}}$. Thus, if $n \gg 1$, the development rate in this region will be well approximated by

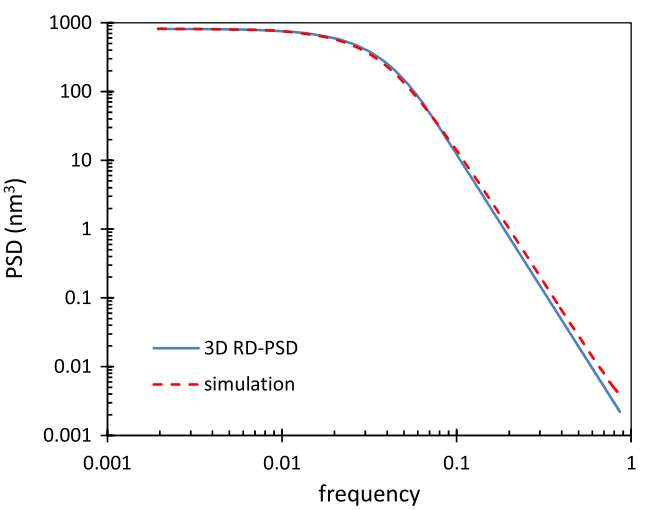

Fig. 2 Example power spectral density (PSD) of development rates generated by the procedure presented in this paper ($\langle m\rangle = 0.73$, $\sigma_m = 0.03$, 1000 trials averaged together), compared to the best fit 3D reaction-diffusion PSD.

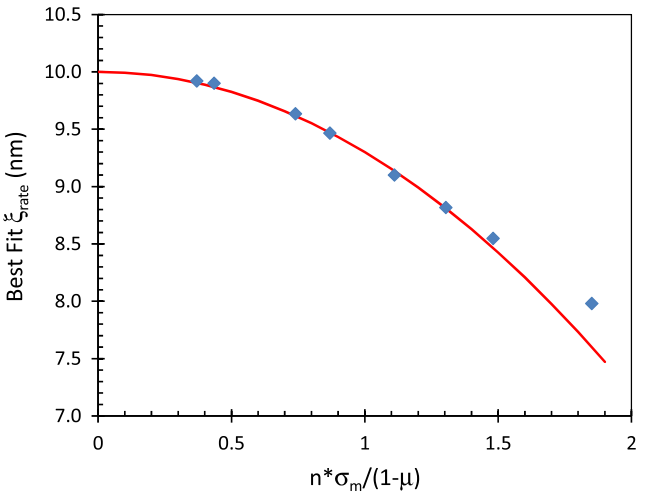

Fig. 3 After calculating the development rate PSD in three dimensions (using $\xi = 10$ nm for the protecting group concentration), an estimate of the resulting development rate correlation length was made by fitting to Eq. (3), shown as the data points (with $\langle m\rangle = 0.73$ and 0.77, σ_m between 0.01 and 0.05, and $n = 10$). A quadratic fit to the data is also shown as the solid line, using the equation $\xi_{\text{rate}} = \xi_m[1 - 0.07(\frac{n\sigma_m}{1-\langle m\rangle})^2]$.

$$r \approx r'_{\max}(1-m)^n, \qquad r'_{\max} = r_{\max}\frac{a+1}{a}. \tag{21}$$

This development rate expression will be used below. While simple, it accurately reflects the non-linear development rate response for the exposure and deprotection levels expected near a photoresist feature edge.

Using the Thorsos method described above, a Gaussian distribution of m with a PSD given by Eqs. (3) and (4) was used in the development rate Eq. (21) to create a random volume of development rate. An example development rate PSD is shown in Fig. 2 ($r_{\max} = 200$ nm/s, $m_{\text{th}} = 0.5$, and $n = 10$).

The shapes of the resultant development rate PSDs are similar to, but not exactly the same as, the PSD function of Eq. (3). By fitting Eq. (3) to the numerical results, the impact of the highly nonlinear development rate function is seen to be a small decrease in the correlation length as a function of the development nonlinearity, n, multiplied by the relative noise in the protecting group concentration, $\sigma_m/(1 - \langle m\rangle)$. Figure 3 shows these results, along with a quadratic fit to the data.

6 Conclusions

The result of the derivations presented in this paper is a simple, new expression for the PSD of the effective acid concentration for a chemically amplified resist. Under conditions of moderately small variations in the protecting group concentration, the PSD of the protecting group concentration also follows this same PSD expression. Finally, near the photoresist line-edge the resulting development rate will also follow this PSD expression (approximately), though with a slightly smaller correlation length. The decrease in the development rate correlation length with increasing development rate noise is a new and unexpected result.

These results can usefully be employed in a comprehensive stochastic model of lithography to predict LER. Previous work to describe the time evolution of rough surfaces

during development has assumed uncorrelated development rate noise.[14] By applying the analytical PSD expressions derived in this paper, future work to simulate the time evolution of developed rough surfaces should show whether kinetic surface roughness caused by dissolution itself dominates the final lithographic roughness or whether the underlying development rate noise, coming from the earlier stochastic reaction-diffusion process, controls the final surface characteristics.

References

1. C. A. Mack, *Fundamental Principles of Optical lithography: The Science of Microfabrication*, pp. 237–252, John Wiley & Sons, London (2007).
2. C. A. Mack et al., "Stochastic exposure kinetics of EUV photoresists: a simulation study," *J. Microlith. Microfab. Microsyst.* **10**(3), 033019 (2011).
3. G. M. Gallatin et al., "Residual speckle in a lithographic illumination system," *J. Microlith. Microfab. Microsyst.* **8**(4), 043003 (2009).
4. O. Noordman et al., "Speckle in optical lithography and its influence on linewidth roughness," *J. Microlith. Microfab. Microsyst.* **8**(4), 043002 (2009).
5. C. A. Mack, "Stochastic modeling in lithography: autocorrelation behavior of catalytic reaction-diffusion systems," *J. Microlith. Microfab. Microsyst.* **8**(2), 029701 (2009).
6. C. A. Mack, "Errata: stochastic modeling in lithography: autocorrelation behavior of catalytic reaction-diffusion systems," *J. Microlith. Microfab. Microsyst.* **11**(2), 029801 (2012).
7. C. A. Mack, *Fundamental Principles of Optical lithography: The Science of Microfabrication*, pp. 228–230, John Wiley & Sons, London (2007).
8. C. A. Mack, "Analytic form for the power spectral density in one, two, and three dimensions," *J. Microlith. Microfab. Microsyst.* **10**(4), 040501 (2011).
9. P. Naulleau and J. Cain, "Experimental and model-based study of the robustness of line-edge roughness metric extraction in the presence of noise," *J. Vac. Sci. Technol.* **B25**(5), 1647–1657 (2007).
10. V. Constantoudis et al., "Line edge roughness and critical dimension variation: fractal characterization and comparison using model functions," *J. Vac. Sci. Technol.* **B22**(4), 1974–1981 (2004).
11. R. L. Stratonovich, *Topics in the Theory of Random Noise*, Vol. I, p. 22, Gordon & Breach, New York (1963).
12. E. I. Thorsos, "The validity of the Kirchhoff approximation for rough surface scattering using a Gaussian roughness spectrum," *J. Accoust. Soc. Am.* **83**(1), 78–92 (1988).
13. C. A. Mack, *Fundamental Principles of Optical lithography: The Science of Microfabrication*, p. 260, John Wiley & Sons, London (2007).
14. C. A. Mack, "Stochastic modeling of photoresist development in two and three dimensions," *J. Microlith. Microfab. Microsyst.* **9**(4), 041202 (2010).

Chris A. Mack developed the lithography simulation software PROLITH and founded and ran the company FINLE Technologies for 10 years. He then served as vice president of lithography technology for KLA-Tencor for five years, until 2005. In 2003, he received the SEMI Award for North America for his efforts in lithography simulation and education, and in 2009 he received the SPIE Frits Zernike Award for Microlithography. He is a fellow of SPIE and IEEE and is also an adjunct faculty member at the University of Texas at Austin. In 2012, he became editor-in-chief of the *Journal of Micro/Nanolithography, MEMS, and MOEMS* (JM^3). Currently, he writes, teaches, and consults on the field of semiconductor microlithography in Austin, Texas.